The Journal of Chemical Physics

Quantum computing for atomic and molecular resonances

Cite as: J. Chem. Phys. **154**, 194107 (2021); https://doi.org/10.1063/5.0040477
Submitted: 14 December 2020 . Accepted: 05 May 2021 . Published Online: 19 May 2021

Teng Bian, and Sabre Kais

The Journal of Chemical Physics ARTICLE scitation.org/journal/jcp

Quantum computing for atomic and molecular resonances

Cite as: J. Chem. Phys. 154, 194107 (2021); doi: 10.1063/5.0040477
Submitted: 14 December 2020 • Accepted: 5 May 2021 •
Published Online: 19 May 2021

Teng Bian and Sabre Kais[a)]

AFFILIATIONS

Department of Chemistry, Purdue University, West Lafayette, Indiana 47907, USA; Department of Physics and Astronomy, Purdue University, West Lafayette, Indiana 47907, USA; and Purdue Quantum Science and Engineering Institute, Purdue University, West Lafayette, Indiana 47907, USA

[a)]Author to whom correspondence should be addressed: kais@purdue.edu

ABSTRACT

The complex-scaling method can be used to calculate molecular resonances within the Born–Oppenheimer approximation, assuming that the electronic coordinates are dilated independently of the nuclear coordinates. With this method, one will calculate the complex energy of a non-Hermitian Hamiltonian, whose real part is associated with the resonance position and imaginary part is the inverse of the lifetime. In this study, we propose techniques to simulate resonances on a quantum computer. First, we transformed the scaled molecular Hamiltonian to second quantization and then used the Jordan–Wigner transformation to transform the scaled Hamiltonian to the qubit space. To obtain the complex eigenvalues, we introduce the direct measurement method, which is applied to obtain the resonances of a simple one-dimensional model potential that exhibits pre-dissociating resonances analogous to those found in diatomic molecules. Finally, we applied the method to simulate the resonances of the H_2^- molecule. The numerical results from the IBM Qiskit simulators and IBM quantum computers verify our techniques.

I. INTRODUCTION

Resonances are intermediate or quasi-stationary states that exist during unique atomic processes such as when an excited atom autoionizes, an excited molecule disassociates unimolecularly, or a molecule attracts an electron and then the ion disassociates into stable ionic and neutral subsystems.[1] The characteristics of resonances, such as energy and lifetime, can be revealed by experiments or predicted by theory. One theoretical method to compute properties associated with such resonances is called the complex-scaling method, developed in Refs. 2–7. This method is based on the Balslev–Combes theorem, which is valid for dilation-analytic potentials and can be extended for non-dilation-analytic potential energies.[8] Additionally, several variants have been developed to study problems such as Stark resonances[9–11] induced by an external electric field. The real space extension of this method uses standard quantum chemistry packages and stabilization graphs.[12] Its main applications are to study the decay of metastable states existing above the ionization threshold of the Li center in open-shell systems such as LiHe,[13] in the computation of transition amplitudes among metastable states,[14] and in explaining Autler–Townes splitting of spectral lines.[15]

The complex-scaling method usually requires a large basis set to predict resonances with good accuracy. For example, the helium ^1S resonance uses 32 Hylleraas type functions for basis construction,[16] and the H_2^- $^2\Sigma_u^+(\sigma_g^2\sigma_u)$ resonance takes a total of 38 constructed Gaussian atomic bases.[8] The computational overhead will become overwhelming if more basis functions need to be considered, such as when simulating larger molecular systems or requiring higher accuracy. Moreover, dimensional scaling and large-order dimensional perturbation theory have been applied for complex eigenvalues using the complex-scaling method.[17,18] As for bound states,[19–23] quantum computing algorithms can overcome the above computational limitation problem for resonances. However, most algorithms cannot be directly adapted to resonance calculation with the complex-scaling method because the complex-rotated Hamiltonian is non-Hermitian. For example, the propagator $e^{-iH(\mathbf{r}e^{i\theta})t}$ in the conventional phase estimation algorithm (PEA) with trotterization[24] will be non-unitary, and it cannot be implemented in

a quantum circuit directly. In this way, a quantum algorithm for resonance calculation that can work with non-Hermitian Hamiltonians is needed. Daskin *et al.*[25] proposed a circuit design that can solve complex eigenvalues of a general non-unitary matrix. The method applies the matrix rows to an input state one by one and estimates complex eigenvalues via an iterative PEA process. However, for molecular Hamiltonians, the gate complexity of this general design is exponential in system size. In our previous publication,[21] we briefly mentioned that our direct measurement method can solve complex eigenvalues of non-Hermitian Hamiltonians with polynomial gates. This study extends the direct measurement method and applies it to simple molecular systems as benchmark tests to obtain resonance properties. In particular, we will use IBM's Qiskit[26] simulators and their quantum computers to calculate these resonances.

In Secs. II–V, we first show how to obtain the complex-scaled Hamiltonian for molecular systems and transform it into the Pauli operator form. Then, we introduce the direct measurement method that can derive the Hamiltonian's complex eigenvalues. Finally, we apply this method to do resonance calculation for a simple model system and a benchmark test system H_2^- using simulators and IBM quantum computers.

II. COMPLEX-SCALED HAMILTONIAN

This section presents the steps needed to convert the complex-rotated Hamiltonian to a suitable form that can be simulated on a quantum computer. In the Born–Oppenheimer approximation, the electronic Hamiltonian of a molecular system can be written as a sum of electronic kinetic energy and potential energy of the form

$$\begin{aligned} H(\mathbf{r}) &= T(\mathbf{r}) + V(\mathbf{r}),\\ T(\mathbf{r}) &= \sum_i -\frac{1}{2}\nabla_i^2,\\ V(\mathbf{r}) &= \sum_{i,j}\frac{1}{|\mathbf{r_i}-\mathbf{r_j}|} + \sum_{i,\sigma}\frac{Z_\sigma}{|\mathbf{r}_i-\mathbf{R}_\sigma|}, \end{aligned} \tag{1}$$

where Z_σ is the σ_{th} nucleus's charge, $\mathbf{R}_\sigma$ is the σ_{th} nucleu's position, and $\mathbf{r}_i$ and $\mathbf{r}_j$ represents the i_{th} and j_{th} electrons' position. The complex-scaling method is applied to the study of molecular resonances within the framework of Born–Oppenheimer approximation. Following Moiseyev *et al.*,[27] the electronic coordinates are dilated independently of the nuclear coordinates. Given such a Hamiltonian $H(\mathbf{r})$ in Eq. (1), where $\mathbf{r}$ represents electrons' coordinates, the complex-scaling method rotates $\mathbf{r}$ into the complex plane by θ, $\mathbf{r}\to\mathbf{r}e^{i\theta}$. Thus, the Hamiltonian becomes $H(\mathbf{r}e^{i\theta})$. After a complex rotation by θ, each electron's position $\mathbf{r}$ becomes $\mathbf{r}/\eta$, where $\eta = e^{-i\theta}$, and thus, the new Hamiltonian from Eq. (1) becomes

$$H_\theta = T(\mathbf{r}/\eta) + V(\mathbf{r}/\eta), \tag{2}$$

$$T(\mathbf{r}/\eta) = \eta^2\sum_i -\frac{1}{2}\nabla_i^2, \tag{3}$$

$$V(\mathbf{r}/\eta) = \eta\sum_{i\neq j}\frac{1}{|\mathbf{r}_i-\mathbf{r}_j|} + \eta\sum_{i,\sigma}\frac{Z_\sigma}{|\mathbf{r}_i-\eta\mathbf{R}_\sigma|}. \tag{4}$$

It is shown that the system's resonance state's energy E and width $\Gamma = \frac{1}{\tau}$, where τ is the life time, are related to the corresponding complex eigenvalue of $H(\mathbf{r}e^{i\theta})$,[3,28]

$$E_\theta = E - \frac{i}{2}\Gamma. \tag{5}$$

When doing exact calculations in an infinite basis limit, E_θ in Eq. (5) is not a function of θ. However, there would be dependence in reality because only a truncated basis set is always used in practice. The best resonance estimate is when the complex energy E_θ pauses or slows down in its trajectory[28,29] in the (E_θ,θ) plane or $\frac{dE_\theta}{d\theta} = 0$. In this way, E and Γ can be obtained by solving the new Hamiltonian's eigenvalues for θ trajectories and looking for the pause. A scaling parameter α is commonly used in the complex rotation process to locate better resonances, which makes $\eta = \alpha e^{-i\theta}$. We refer the readers to the book on non-Hermitian quantum mechanics by Moiseyev for more details and method applications.[27]

After choosing a proper orthogonal basis set $\{\psi_i(\mathbf{r})\}$, the Hamiltonian can be converted into a second-quantization form,

$$H_\theta = \sum_{i,j} h_{ij}a_i^\dagger a_j + \frac{1}{2}\sum_{i,j,k,l} h_{ijkl}a_i^\dagger a_j^\dagger a_k a_l. \tag{6}$$

In the equation, $a_i^\dagger$ and a_i are fermionic creation and annihilation operators. The coefficients h_{ij} and h_{ijkl} can be calculated by

$$\begin{aligned} h_{ij} &= \int \psi_i^*(\mathbf{r})\left(-\eta^2\frac{1}{2}\nabla_i^2 + \eta\sum_\sigma\frac{Z_\sigma}{|\mathbf{r}-\eta\mathbf{R}_\sigma|}\right)\psi_j(\mathbf{r}),\\ h_{ijkl} &= \int \psi_i^*(\mathbf{r_1})\psi_j^*(\mathbf{r_2})\frac{\eta}{|\mathbf{r}_1-\mathbf{r}_2|}\psi_k(\mathbf{r_2})\psi_l(\mathbf{r_1}). \end{aligned} \tag{7}$$

With the Jordan–Wigner transformation,[30]

$$\begin{aligned} a_j^\dagger &= \frac{1}{2}(X_j - iY_j)\otimes\overrightarrow{Z_{j-1}},\\ a_j &= \frac{1}{2}(X_j + iY_j)\otimes\overrightarrow{Z_{j-1}}, \end{aligned} \tag{8}$$

in which X, Y, and Z are the Pauli operators and

$$\overrightarrow{Z_{j-1}} = Z_{j-1}\otimes Z_{j-2}\otimes Z_0, \tag{9}$$

and the Hamiltonian in Eq. (6) will be further transformed into Pauli operators as

$$H_\theta = \sum_{i=0}^{L-1} c_i P_i. \tag{10}$$

In the summation, c_i represents a complex coefficient and P_i represents a k-local tensor product of Pauli operators, where $k \le n$ and n is the size of the basis set. Alternatively, the Bravyi–Kitaev transformation[30] or parity transformation can also be used in the final step for obtaining the Hamiltonian in the qubit space.

The above process is the same as the conventional Hamiltonian derivation in quantum computing for electronic structure

calculations of bound states.[19,31–34] Here, for resonance calculations, to make the Hamiltonian more compatible with the direct measurement method, we rewrite Eq. (10) as

$$H_\theta = \sum_{i=0}^{2^{n_a}-1} \beta_i V_i, \tag{11}$$

where $n_a = \lceil \log_2 L \rceil$. The coefficient β_i and the operator V_i are determined in the following ways:

$$\begin{aligned} \beta_i = |c_i|, V_i = \frac{c_i}{|c_i|} P_i \quad \text{when } i < L, \\ \beta_i = 0, V_i = I \quad \text{when } i \geq L. \end{aligned} \tag{12}$$

III. DIRECT MEASUREMENT METHOD

The direct measurement method is inspired by the direct application of the phase estimation algorithm[35] as briefly discussed in our previous publication.[21] Here, the basic idea is to apply the complex-rotated Hamiltonian to the state of the molecular system and obtain the complex energy information from the output state. Since the original non-Hermitian Hamiltonian cannot be directly implemented in a quantum circuit, this direct measurement method embeds it into a larger dimensional unitary operator.

Assuming n spin orbitals need to be considered for the system, the direct measurement method requires $n_s = n$ qubits to prepare the state of the model system $|\phi_r\rangle_s$ and an extra n_a ancilla qubits to enlarge the non-Hermitian Hamiltonian to be a unitary operator. The quantum circuit is shown in Fig. 1.

The B and V gates in the circuit are designed to have the following properties:

$$B|0\rangle_a = \sum_{i=0}^{2^{n_a}-1} \sqrt{\frac{\beta_i}{A}} |i\rangle_a, \quad A = \sum_{i=0}^{2^{n_a}-1} \beta_i, \tag{13}$$

$$V|i\rangle_a|\phi_r\rangle_s = |i\rangle_a V_i|\phi_r\rangle_s, \tag{14}$$

which means B transforms the initial ancilla qubits' state to a vector of coefficients and V applies all V_i on system qubits based on ancilla qubits' states. One construction choice for B could be implementing the unitary operator

$$B = 2\left(\sum_{i=0}^{2^{n_a}-1} \sqrt{\frac{\beta_i}{A}} |i\rangle_a\right)\left(\sum_{i=0}^{2^{n_a}-1} \sqrt{\frac{\beta_i}{A}} \langle i|_a\right) - I. \tag{15}$$

As for V, a series of multi-controlled V_i gates will do the work. If $|\phi_r\rangle_s$ is chosen as an eigenstate and we apply the whole circuit of B, V, and $B^\dagger$,

$$U_r = \left(B^\dagger \otimes I^{\otimes n_s}\right) V \left(B \otimes I^{\otimes n_s}\right), \tag{16}$$

on it, the output state will be

$$U_r|0\rangle_a|\phi\rangle_s = \frac{Ee^{i\varphi}}{A}|0\rangle_a|\phi\rangle_s + |\Phi^\perp\rangle, \tag{17}$$

where $Ee^{i\varphi}$ $(E \geq 0)$ is the corresponding eigenvalue and $|\Phi^\perp\rangle$ is a state whose ancilla qubits' state is perpendicular to $|0\rangle_a$. Then, we can derive E by measuring the output state. To obtain the phase φ, we apply a similar circuit for $H'_\theta = xI^{\otimes n} + H_\theta$, where x is a selected real number, and perform the measurements. The calculation details are found in Appendix C.

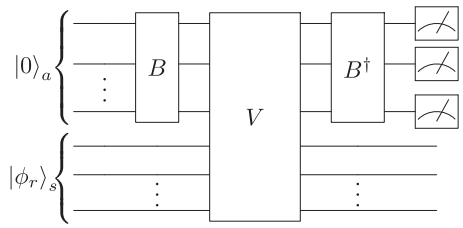

FIG. 1. The quantum circuit for the direct measurement method. B and V gates are constructed based on the coefficients and operators in Eq. (11). The system qubits' state and ancilla qubits' state are initialized as $|0\rangle_a$ and $|\phi_r\rangle_s$, respectively.

IV. QUANTUM SIMULATION OF RESONANCES IN A SIMPLE MODEL SYSTEM

In this section, we calculate the resonance properties of a model system using the direct measurement method. This system is the following one-dimensional potential:[28]

$$V(x) = \left(\frac{1}{2}x^2 - J\right)e^{-\lambda x^2} + J. \tag{18}$$

Parameters are chosen as $\lambda = 0.1$ and $J = 0.8$. The potential plot is in Fig. 2. This potential is used to model some resonance phenomena in diatomic molecules. We only consider one electron under this potential. The original Hamiltonian and the complex-rotated Hamiltonian can be written as

$$H = -\frac{\nabla_x^2}{2} + V(x), \tag{19}$$

$$H_\theta = -\eta^2 \frac{\nabla_x^2}{2} + V(\eta x). \tag{20}$$

To make the setting consistent with the original literature, η is chosen to be $e^{-i\theta}$ and the scaling parameter α is embedded in n Gaussian basis functions

$$\chi_k(\alpha) = \exp(-\alpha_k x^2), \tag{21}$$

$$\alpha_k = \alpha(0.45)^k, \quad k = 0, 1, \ldots, n-1. \tag{22}$$

The $\{\chi_k(\alpha)\}$ basis set is not orthogonal, so we apply the Gram–Schmidt process and iteratively construct an orthogonal basis set $\{\psi_i\}$ as follows:

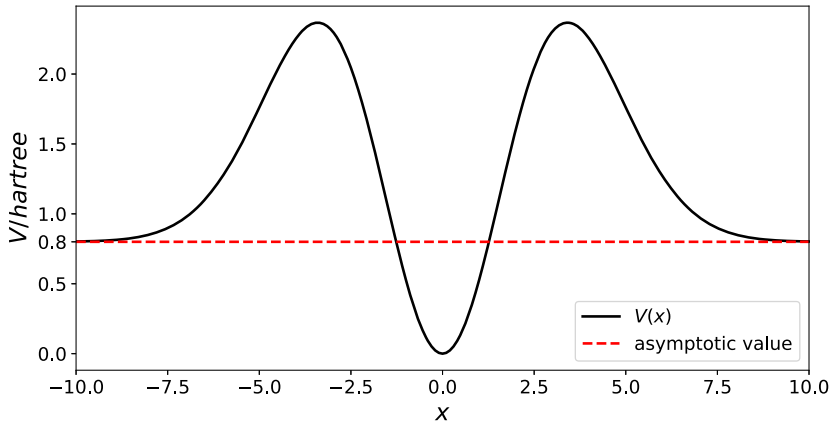

FIG. 2. The one-dimensional potential $V(x) = (\frac{1}{2}x^2 - J)e^{-\lambda x^2} + J$, where $\lambda = 0.1$ and $J = 0.8$.

$$\gamma_k = \chi_k - \sum_{i=0}^{k-1} \langle \chi_k | \psi_i \rangle \psi_i, \tag{23}$$

$$\psi_i = \frac{\gamma_k}{\|\gamma_k\|} = \frac{\gamma_k}{\sqrt{\langle \gamma_k | \gamma_k \rangle}}. \tag{24}$$

Since there is only one electron, we do not consider spin interactions. This $\{\psi_i\}$ basis set is used in the second-quantization step to get the final Hamiltonian in the Pauli matrix form. The resonance eigenvalue found in Ref. 28 with $n = 10$ basis functions is $E_\theta = 2.124 - 0.019i$ hartree. We will try to get the same resonance by applying the direct measurement method using the Qiskit package. The Qiskit package supports different backends, including a statevector simulator that executes ideal circuits, a QASM simulator that provides noisy gate simulation, and various quantum computers. In what follows, we show the results when the basis function

TABLE I. The number of qubits and estimated gates in different cases when the direct measurement method is used to calculate the resonance properties of the model system. The estimation for gate numbers is based on the QASM simulator and IBM machines.

Case name	Number of basis functions	Number of total qubits	Number of system qubits	Number of ancilla qubits	Number of gates
C1	5	10	5	5	$\sim 10^6$
C2	2	5	2	3	~800
C3	2	4	2	2	~200
C4	2	3	2	1	~10

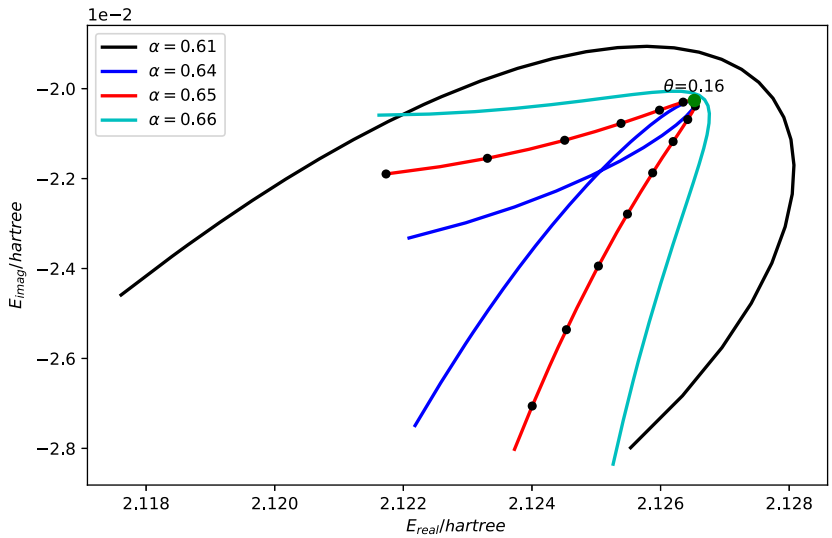

FIG. 3. Trajectories of a complex eigenvalue on the rotation angle θ for fixed $n = 5$ and various α, calculated by the Qiskit statevector simulator. θ ranges from 0.1 to 0.24 with a step of 0.01. The green point shows the best estimation of resonance energy, which is $E = 2.1265 - 0.0203i$ hartree, that occurs at $\alpha = 0.65$ and $\theta = 0.160$. The input state for the direct measurement method is obtained by directly diagonalizing the complex-rotated Hamiltonian matrix.

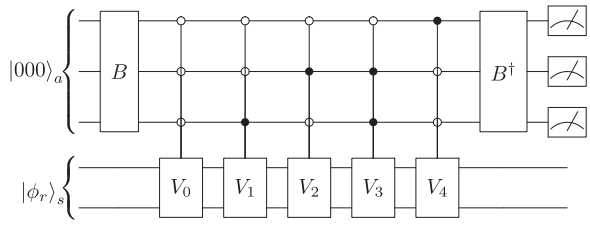

FIG. 4. The quantum circuit to run the direct measurement method when $n = 2$. The B gate is prepared by the coefficients [1.315 56, 0.13 333, 0.133 33, 0.252 12, 1.063 78]. V_0, V_1, V_2, V_3, and V_4 are applying $e^{-0.041\,80i}II$, $e^{2.328\,88i}YY$, $e^{2.328\,88i}XX$, $e^{3.052\,83i}ZI$, and $e^{3.110\,93i}IZ$, respectively.

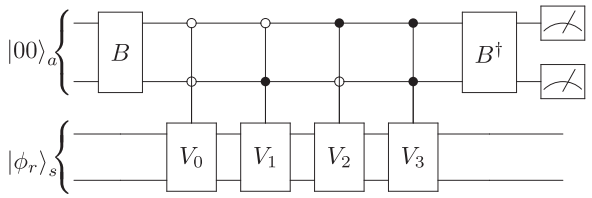

FIG. 5. The simplified quantum circuit to run the direct measurement method when $n = 2$. The B gate is prepared by the coefficients [0.133 33, 0.133 33, 0.252 12, 1.063 78]. V_0, V_1, V_2, and V_3 are applying $e^{2.328\,88i}YY$, $e^{2.328\,88i}XX$, $e^{3.052\,83i}ZI$, and $e^{3.110\,93i}IZ$, respectively.

number is $n = 5$ and $n = 2$. In particular, the former $n = 5$ case shows how θ trajectories locate the best resonance estimate, and the latter $n = 2$ cases show how to further simplify the quantum circuit for the direct measurement method and run it on IBM quantum computers.

C1 in Table I is our primary example where we follow the above steps in Secs. II and III for $n = 5$. An example of the complex-rotated Hamiltonian is shown in Appendix A. Figure 3 shows a sweep of scaling parameters α for statevector simulations of θ trajectories. Most trajectories pause around the point, $E_\theta = 2.1265 - 0.0203i$ hartree, when $\alpha = 0.65$ and $\theta = 0.160$. Based on Eq. (5), this indicates that the resonance energy and width are $E = 2.1265$ hartree and $\Gamma = 0.0406$ hartree, respectively, close to the resonance energy from Ref. 28 The IBM quantum computer cannot perform the method due to a large number of standard gates in the circuit. Instead, we used the QASM simulator for $4 * 10^4$ shots and obtained the system's resonance energy at $\alpha = 0.65$, $\theta = 0.160$, and $E_\theta = 2.1005 - 0.3862i$ hartree. This result has an error of around 0.3 hartree but can be augmented by more sample measurements.

When taking $n = 2$ for the basis function, we are not able to locate the best resonance estimate (see Fig. 3) based on direct diagonalization. Hence, we only use the direct measurement method to calculate the complex eigenenergy when $\alpha = 0.65$ and $\theta = 0.160$, where the best location is at $n = 5$. We run the direct measurement method using simulators first and then try to reduce the number of ancilla qubits to make the resulting circuit short enough to be executed in the IBM quantum computers.

C2 in Table I is the case when we follow the steps for $n = 2$ in Secs. II and III. The Hamiltonian H_θ and how to calculate its complex eigenvalue are shown in Appendix D 1 [Eq. (D1)]. Figure 4 gives the quantum circuit for H_θ. This circuit can be executed in simulators with the results listed in Table II.

TABLE II. The complex eigenenergy obtained by directly diagonalizing the Hamiltonian and by running different simulators. The QASM simulator is configured to have no noise, and it takes 10^5 samples to calculate the complex eigenenergy.

Method	Eigenenergy (hartree)	Error (hartree)
Direct diagonalization	2.1259 − 0.1089i	⋯
Statevector simulator	2.1259 − 0.1089i	0
QASM simulator	2.1279 − 0.1100i	2×10^{-3}

However, it is too complicated to be successfully run in IBM quantum computers. For C3 in Table I, we simplify the quantum circuit by calculating the complex eigenvalue for the Hamiltonian H_θ in Appendix D 2 [Eq. (D3)]. Because there are only four terms left, two ancilla qubits are enough for the method. The simplified quantum circuit is then shown in Fig. 5. To avoid introducing more ancilla qubits, instead of $H'_\theta = H_\theta + xII$, we can run a similar four-qubit circuit for $H'_\theta = H_\theta + H^3_\theta$, which has the same terms of tensor products as H_θ with different coefficients. This circuit can be executed successfully in the simulators and the IBM quantum computers. However, it costs around 200 gates in the IBM quantum computers, leading to a significant error. The resulting resonance eigenenergies and errors can be seen in Table III.

For the Hamiltonian in Eq. (D3), a simpler circuit can be constructed if we try to calculate the complex eigenvalue of its square [Eq. (D6) in Appendix D 3]. This is C4 in Table I. The quantum circuit for this H^2_θ is shown in Fig. 6.

We can also run a similar three-qubit circuit for $(H^2_\theta)' = H^2_\theta + H^4_\theta$. The implementation of the circuit costs nine gates in the

TABLE III. The complex eigenenergy obtained by directly diagonalizing the Hamiltonian, running simulators and using IBM quantum computers. The QASM simulator is configured to be noiseless, and it takes 10^5 samples to calculate the complex eigenenergy. The IBM quantum computer takes 2^{13} samples.

Method	Eigenenergy (hartree)	Error (hartree)
Direct diagonalization	2.1259 − 0.1089i	⋯
Statevector simulator	2.1259 − 0.1089i	0
QASM simulator	2.1264 − 0.1099i	1×10^{-3}
IBM quantum computer	2.0700 − 0.4890i	0.3841

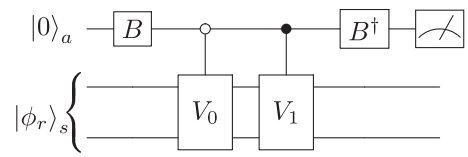

FIG. 6. The quantum circuit to run the direct measurement method when $n = 2$. The B gate is prepared by the coefficients [1.195 77, 0.535 29]. V_0 and V_1 are applying $e^{-0.09723i}II$ and $e^{-0.05311i}ZZ$, respectively.

TABLE IV. The complex eigenenergy obtained by directly diagonalizing the Hamiltonian, running simulators and running IBM quantum computers. The QASM simulator is configured to be noiseless, and it takes 10^5 samples to calculate the complex eigenenergy. The IBM quantum computer takes 2^{13} samples. The error of the IBM quantum computer is from the best case.

Method	Eigenenergy (hartree)	Error (hartree)
Direct diagonalization	2.1259 − 0.1089i	⋯
Statevector simulator	2.1259 − 0.1089i	0
QASM simulator	2.1259 − 0.1107i	1.70×10^{-3}
IBM quantum computer	2.1624 − 0.1188i	0.0378

IBM quantum computers after circuit optimization. The resulting eigenenergies are in Table IV.

V. QUANTUM SIMULATION OF THE RESONANCES IN H_2^-

This section presents a proof of concept that by using our quantum algorithm, the direct measurement method, one can calculate molecular resonances on a quantum computer. We focus on the resonances of a simple diatomic molecule, H_2^- $^2\Sigma_u^+(\sigma_g^2\sigma_u)$. Moiseyev and Corcoran[8] showed how to obtain this molecule's resonance using a variational method based on the (5s, 3p, 1d/3s, 2p, 1d) contracted Gaussian atomic basis, which contains a total of 76 atomic orbitals for H_2^-. They picked around 45 configurations of natural orbitals as a final basis for the resonance calculation. Here, however, we are not going to use their contracted Gaussian atomic basis that needs 76 system qubits with additional ancilla qubits, which is too large to be simulated by classical computers. The number of gates would also be overwhelming. One may try an iterative diagonalization approach to get a few eigenvalues without constructing matrices or vectors. Another possible solution could be using tensor network simulators. Recent studies by Ellerbrock and Martinez show that tensor network simulators are able to efficiently and accurately simulate over 100-qubit circuits with moderate entanglement.[36] In another study, Zhou *et al.* showed that even strongly entangled systems (as those generated by 2D random circuits) can be simulated by matrix product states comparably accurate to modern quantum devices.[37] However, building those simulators for our system is beyond the scope of this paper. In this way, we picked small basis sets, 6-31g and cc-pVDZ, for our simulations. We used the Born–Oppenheimer approximation followed by complex rotation, as shown in Sec. II, "COMPLEX-SCALED HAMILTONIAN" and mapped the Hamiltonian to the qubit space, as shown in Appendix B. We then apply the direct measurement method to the Hamiltonian to obtain complex eigenvalues. An example quantum circuit to run the direct measurement method can be found in Appendix E.

Figure 7 shows one complex eigenvalue's θ trajectories at $\alpha = 1.00$ under different basis sets after running the algorithm. Figure 7(a) is simulated using the 6-31g basis set. Eight spin orbitals are considered in our self-defined simulator, and 16 qubits are needed to run the algorithm. In this case, if we fix $\eta = \alpha e^{-i\theta}$ at the lowest point in the figure, which has $\alpha = 1.00$, $\theta = 0.18$, the resonance energy obtained by the direct measurement method is $E_\theta = -0.995\,102 - 0.046\,236i$ hartree. This complex energy is close to that obtained in Ref. 8, $E_\theta = -1.0995 - 0.0432i$ hartree, especially the imaginary part. Figure 7(b) is simulated using the cc-pVDZ basis set. We only considered the s and p_z basis functions for H atoms for easier simulation. 12 spin orbitals are considered in our self-defined simulator, and a total of 23 qubits are needed to run the algorithm in quantum computers. The results show that the resonance energy at the lowest point in the figure, which has $\alpha = 1.00$, $\theta = 0.22$, is $E_\theta = -1.045\,083 - 0.044\,513i$ hartree. This is even closer to that obtained in Ref. 8. However, we want to note that the lowest points in Figs. 7(a) and 7(b) are not pause points. In addition, they do not reveal real resonance properties. Even after shifting

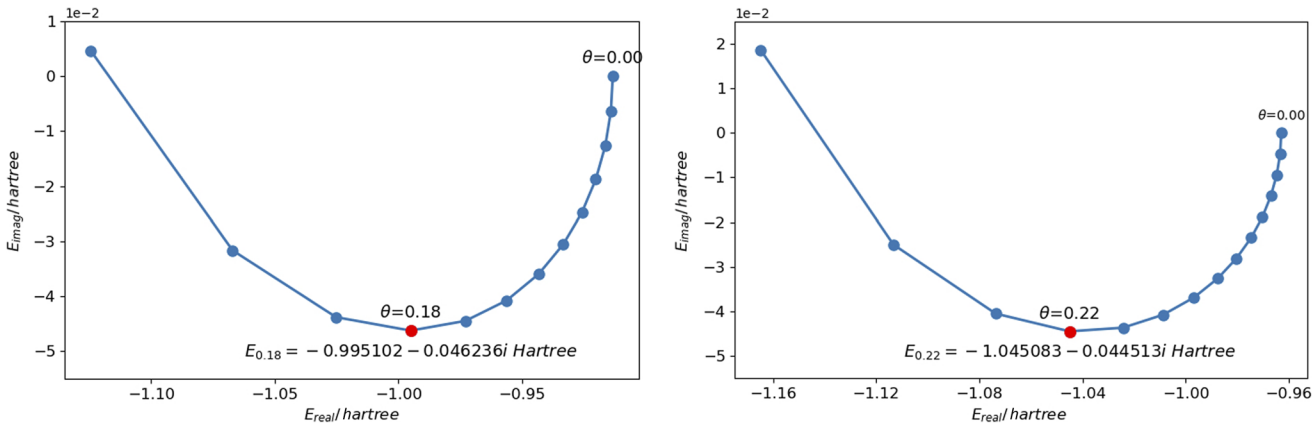

FIG. 7. Complex eigenvalue trajectories on the rotation angle θ at $\alpha = 1.00$ for molecule H_2^- calculated by a self-defined simulator. (a) uses the 6-31g basis set for H atoms, including 1s and 2s orbitals. θ ranges from 0.00 to 0.24 with a step of 0.02. At the lowest point when $\theta = 0.18$, the complex eigenvalue is $-0.995\,102 - 0.046\,236i$ hartree. (b) uses the s and p_z orbitals in the cc-pVDZ basis set for H atoms. θ ranges from 0.00 to 0.28 with a step of 0.02. At the lowest point when $\theta = 0.22$, the complex eigenvalue is $-1.045\,083 - 0.044\,513i$ hartree.

different α in simulations, we cannot find a consistent pause point in θ trajectories to locate the best resonance estimation. The reason may be related to our selected basis. Compared with the literature,[8] our basis set is much smaller and is not optimized for the resonance state. Still, this application gives a proof of concept and shows that one can calculate molecular resonances on a quantum computer. In the future, if more qubits are available in quantum computers, a large basis can be used, and we may be able to show finer structures in trajectories that can locate the best resonance point. In addition, a larger basis set should lead to a more accurate resonance calculation.

VI. CONCLUSION

In this paper, we construct and show a proof of concept for a quantum algorithm that calculates atomic and molecular resonances. We first presented the complex-scaling method to calculate molecular resonances. Then, we introduced the direct measurement method, which embeds a molecular system's complex-rotated Hamiltonian into the quantum circuit and calculates the resonance energy and lifetime from the measurement results. These results represent the first applications of the complex-scaling Hamiltonian to molecular resonances on a quantum computer. The method is proven to be accurate when applied to a simple one-dimensional quantum system that exhibits shape resonances. We tested our algorithm on quantum simulators and IBM quantum computers. Furthermore, when compared to the exponential time complexity in traditional matrix-vector multiplication calculations, this method only requires $O(n^5)$ standard gates, where n is the size of the basis set. These findings show this method's potential to be used in a more complicated molecular system and for better accuracy in the future when more and better qubit machines are available.

ACKNOWLEDGMENTS

We would like to thank Rongxin Xia, Zixuan Hu, and Manas Sajjan for useful discussions. We also like to acknowledge financial support from the National Science Foundation under Award No. 1955907.

APPENDIX A: COMPLEX-ROTATED HAMILTONIAN OF THE MODEL SYSTEM AT $\theta = 0.16$, $\alpha = 0.65$ WHEN $n = 5$

Table V shows an example of the model system's complex-rotated Hamiltonian.

APPENDIX B: COMPLEX-ROTATED HAMILTONIAN OF H_2^- AT $\theta = 0.18$, $\alpha = 1.00$

Table VI shows an example of the H_2^- system's complex-rotated Hamiltonian.

TABLE V. The coefficients and tensor product operators of the model system's complex-rotated Hamiltonian H_θ at $\theta = 0.16$, $\alpha = 0.65$ when there is $n = 5$ basis functions.

YYIII	$-0.091\,665 + 0.096\,819i$	XXIII	$-0.091\,665 + 0.096\,819i$	IIIII	$4.599\,205 - 0.533\,073i$
ZIIII	$-0.251\,131 + 0.022\,353i$	YZYII	$0.017\,915\,6 - 0.030\,997i$	XZXII	$0.017\,915\,6 - 0.030\,997i$
YZZYI	$-0.007\,005 + 0.015\,446i$	XZZXI	$-0.007\,005 + 0.015\,446i$	YZZZY	$0.003\,680 - 0.009\,152i$
XZZZX	$0.003\,680 - 0.009\,152i$	IZIII	$-1.063\,280 + 0.032\,614i$	IYYII	$-0.089\,297 + 0.108\,259i$
IXXII	$-0.089\,297 + 0.108\,259i$	IYZYI	$0.014\,213 - 0.055\,870i$	IXZXI	$0.014\,213 - 0.055\,870i$
IYZZY	$-0.003\,869 + 0.033\,693i$	IXZZX	$-0.003\,869 + 0.033\,693i$	IIZII	$-1.445\,349 + 0.113\,618i$
IIYYI	$-0.209\,952 + 0.010\,748i$	IIXXI	$-0.209\,952 + 0.010\,748i$	IIYZY	$0.060\,302 - 0.008\,776j$
IIXZX	$0.060\,302 - 0.008\,776i$	IIIZI	$-1.127\,058 + 0.243\,702i$	IIIYY	$-0.336\,956 + 0.051\,691i$
IIIXX	$-0.336\,956 + 0.051\,691i$	IIIIZ	$-0.712\,385 + 0.120\,784i$		

TABLE VI. The coefficients and tensor product operators in H_2^-'s complex-rotated Hamiltonian at $\theta = 0.18$, $\alpha = 1.00$ when using the 6-31g basis set.

IXZXXZXI	$0.018\,705 - 0.003\,404i$	IIIZIXZX	$0.038\,191 - 0.006\,950i$	ZIZIIIII	$0.103\,932 - 0.018\,913i$
XZXIXZXI	$0.027\,826 - 0.005\,063i$	IXXIIIXX	$-0.002\,794 + 0.000\,508i$	IIZZIIII	$0.106\,657 - 0.019\,408i$
IYIYIIII	$0.024\,307 - 0.004\,423i$	IIIIXXXX	$0.015\,119 - 0.002\,751i$	IZIIIIZI	$0.095\,226 - 0.017\,328i$
IIIIIIXX	$0.047\,512 - 0.039\,979i$	YYIIYZZY	$-0.019\,254 + 0.003\,504i$	XZXIYZYI	$0.027\,826 - 0.005\,063i$
IZIIYZYI	$0.013\,080 - 0.002\,380i$	IIYYIIXX	$0.034\,554 - 0.006\,288i$	XZXIIIZI	$0.032\,587 - 0.005\,930i$
YYYYIIII	$0.015\,119 - 0.002\,751i$	XXIIIYYI	$0.005\,216 - 0.000\,949i$	IXIXIIII	$0.024\,307 - 0.004\,423i$
IIIIXXYY	$0.002\,918 - 0.000\,531i$	IIIZXZXI	$0.050\,249 - 0.009\,144i$	IIXXXXII	$0.020\,481 - 0.003\,727i$
YYIIYYII	$0.019\,597 - 0.003\,566i$	IXXIIXXI	$0.008\,283 - 0.001\,507i$	IIIIXIXI	$0.016\,733 - 0.003\,045i$
IYZYIIII	$-0.035\,671 + 0.030\,324i$	IYZYIIIZ	$0.043\,018 - 0.007\,828i$	YYIIIYYI	$0.005\,216 - 0.000\,949i$
IIIIXZZX	$-0.028\,316 + 0.033\,738i$	XXIIYYII	$0.019\,597 - 0.003\,566i$	IXXIIIYY	$-0.002\,794 + 0.000\,508i$

TABLE VI. (*Continued.*)

ZYZYIIII	0.015 436 − 0.002 809*i*	XXIIYZZY	−0.019 254 + 0.003 504*i*	IIIIIZZI	0.084 620 − 0.015 398*i*
YZYIIZII	0.011 702 − 0.002 129*i*	IIYYXZZX	−0.031 698 + 0.005 768*i*	IIIIIXXI	−0.007 550 + 0.006 494*i*
IXZXIZII	0.012 371 − 0.002 251*i*	IIIIYYYY	0.015 119 − 0.002 751*i*	IIIZYZYI	0.050 249 − 0.009 144*i*
ZIIIIIII	−0.230 405 + 0.108 639*i*	ZIIIIIIZ	0.159 054 − 0.028 943*i*	IXXIYZZY	0.006 593 − 0.001 200*i*
IIIIIYIY	0.023 153 − 0.004 213*i*	IIYYIXXI	−0.000 541 + 0.000 098*i*	YZZYIIII	−0.027 204 + 0.031 862*i*
IIIZIIZI	0.139 579 − 0.025 399*i*	YZZYXXII	−0.016 647 + 0.003 029*i*	IIXXIIII	0.047 746 − 0.040 370*i*
XIXIIIII	0.017 118 − 0.003 115*i*	YYIIXXII	0.019 597 − 0.003 566*i*	YZYIIYZY	0.017 127 − 0.003 117*i*
IIIIZZII	0.084 496 − 0.015 376*i*	YZZYXZZX	0.031 161 − 0.005 670*i*	IIZIIYZY	0.024 717 − 0.004 498*i*
XZZXIXXI	0.004 990 − 0.000 908*i*	IYYIIYYI	0.008 283 − 0.001 507*i*	IYZYIXZX	0.015 728 − 0.002 862*i*
XZZXXZZX	0.031 161 − 0.005 670*i*	IYZYIIZI	0.026 040 − 0.004 739*i*	IIZIIZII	0.093 507 − 0.017 015*i*
IZIIZIII	0.106 161 − 0.019 318*i*	XXIIIXXI	0.005 216 − 0.000 949*i*	IXZXIYZY	0.015 728 − 0.002 862*i*
ZIIIIXZX	0.030 922 − 0.005 627*i*	IIIIIIYY	0.047 512 − 0.039 979*i*	XXIIIIYY	0.021 209 − 0.003 859*i*
XXIIIIXX	0.021 209 − 0.003 859*i*	YYIIIIII	0.001 646 − 0.022 572*i*	ZIIIIIZI	0.130 169 − 0.023 687*i*
IIYYIIYY	0.034 554 − 0.006 288*i*	YZYIIIIZ	0.052 229 − 0.009 504*i*	YZYIIIII	−0.021 561 + 0.077 956*i*
IIXXXZZX	−0.031 698 + 0.005 768*i*	IIIIZYZY	0.013 729 − 0.002 498*i*	IYYIXXII	0.003 919 − 0.000 713*i*
IIZIZIII	0.133 407 − 0.024 276*i*	YZZYYZZY	0.031 161 − 0.005 670*i*	XZXIZIII	0.040 337 − 0.007 340*i*
ZIIIZIII	0.151 365 − 0.027 544*i*	YZYIIXZX	0.017 127 − 0.003 117*i*	IIIIYIYI	0.016 733 − 0.003 045*i*
IIXXIYYI	−0.000 541 + 0.000 098*i*	IIYYYZZY	−0.031 698 + 0.005 768*i*	IYYIIIII	−0.009 705 + 0.008 779*i*
YZZYYYII	−0.016 647 + 0.003 029*i*	XZXIIXZX	0.017 127 − 0.003 117*i*	IIIIIXIX	0.023 153 − 0.004 213*i*
IIZIYZYI	0.033 580 − 0.006 110*i*	ZXZXIIII	0.015 436 − 0.002 809*i*	YZYZIIII	0.020 644 − 0.003 757*i*
IIIIYZZY	−0.028 316 + 0.033 738*i*	IXZXZIII	0.034 152 − 0.006 215*i*	YZZYIYYI	0.004 990 − 0.000 908*i*
ZIIZIIII	0.126 456 − 0.023 011*i*	YZZYIIXX	−0.029 557 + 0.005 379*i*	XZZXYZZY	0.031 161 − 0.005 670*i*
IYYIIIYY	−0.002 794 + 0.000 508*i*	IXZXIIII	−0.035 671 + 0.030 324*i*	IXZXIIIZ	0.043 018 − 0.007 828*i*
ZIIIYZYI	0.038 659 − 0.007 035*i*	IIXXIIXX	0.034 554 − 0.006 288*i*	ZZIIIIII	0.085 046 − 0.015 476*i*
IIIZZIII	0.158 431 − 0.028 830*i*	YXXYIIII	0.012 162 − 0.002 213*i*	IZIIIYZY	0.013 159 − 0.002 395*i*
IYZYXZXI	0.018 705 − 0.003 404*i*	XXIIXXII	0.019 597 − 0.003 566*i*	IIIIYXXY	0.012 201 − 0.002 220*i*
IIIIZIII	−0.231 557 + 0.112 195*i*	IIIIZIIZ	0.128 680 − 0.023 416*i*	YZYIXZXI	0.027 826 − 0.005 063*i*
IIYYYYII	0.020 481 − 0.003 727*i*	IIIIXZXZ	0.020 604 − 0.003 749*i*	IIIIXZXI	−0.030 067 + 0.081 498*i*
IIYYIYYI	−0.000 541 + 0.000 098*i*	IYYIYZZY	0.006 593 − 0.001 200*i*	YZYIYZYI	0.027 826 − 0.005 063*i*
IIZIXZXI	0.033 580 − 0.006 110*i*	IIXXYZZY	−0.031 698 + 0.005 768*i*	IIIIIIZI	−0.611 815 + 0.267 480*i*
IIIIIIZZ	0.107 859 − 0.019 627*i*	YZZYIXXI	0.004 990 − 0.000 908*i*	IIIIIXZX	−0.012 982 + 0.018 373*i*
XXIXXII	0.003 919 − 0.000 713*i*	IIZIIIII	−0.612 966 + 0.271 036*i*	XZXIIYZY	0.017 127 − 0.003 117*i*
IIXXIXXI	−0.000 541 + 0.000 098*i*	IIIIYYII	0.000 598 − 0.021 276*i*	YYIIIIXX	0.021 209 − 0.003 859*i*
XZZXYYII	−0.016 647 + 0.003 029*i*	XZXZIIII	0.020 644 − 0.003 757*i*	YZZYIIYY	−0.029 557 + 0.005 379*i*
YYXXIIII	0.002 957 − 0.000 538*i*	YZYIIIZI	0.032 587 − 0.005 930*i*	IIXXYYII	0.020 481 − 0.003 727*i*
IXZXIXZX	0.015 728 − 0.002 862*i*	IXZXIIZI	0.026 040 − 0.004 739*i*	XYYXIIII	0.012 162 − 0.002 213*i*
ZIIIXZXI	0.038 659 − 0.007 035*i*	IIXXIIYY	0.034 554 − 0.006 288*i*	YYIIIIYY	0.021 209 − 0.003 859*i*
IZZIIIII	0.087 497 − 0.015 922*i*	IZIIIZII	0.094 105 − 0.017 124*i*	IIYYXXII	0.020 481 − 0.003 727*i*
IIIZIYZY	0.038 191 − 0.006 950*i*	IYYIIIXX	−0.002 794 + 0.000 508*i*	IXXIXZZX	0.006 593 − 0.001 200*i*
IIIIZXZX	0.013 729 − 0.002 498*i*	IIIIIYYI	−0.007 550 + 0.006 494*i*	IIIIZIZI	0.103 932 − 0.018 913*i*
YYIIXZZX	−0.019 254 + 0.003 504*i*	IXXIIIII	−0.009 705 + 0.008 779*i*	IIIIXXII	0.000 598 − 0.021 276*i*
XZZXIYYI	0.004 990 − 0.000 908*i*	IZIIIIIZ	0.110 454 − 0.020 099*i*	IZIIIIII	−0.388 873 + 0.102 313*i*
IYZYIZII	0.012 371 − 0.002 251*i*	IXXIIYYI	0.008 283 − 0.001 507*i*	IYYIYYII	0.003 919 − 0.000 713*i*
YYIIIXXI	0.005 216 − 0.000 949*i*	XXYYIIII	0.002 957 − 0.000 538*i*	IXXIYYII	0.003 919 − 0.000 713*i*
IIIIYZYZ	0.020 604 − 0.003 749*i*	IIIIYZYI	−0.030 067 + 0.081 498*i*	IYZYIYZY	0.015 728 − 0.002 862*i*
IZIIXZXI	0.013 080 − 0.002 380*i*	IIIIIIII	1.734 311 − 1.110 499*i*	IIIIIIIZ	−0.896 247 + 0.369 556*i*
IIZIIXZX	0.024 717 − 0.004 498*i*	IZIIIXZX	0.013 159 − 0.002 395*i*	IIZIIIZI	0.120 598 − 0.021 945*i*
XZZXIIYY	−0.029 557 + 0.005 379*i*	IIIIXYYX	0.012 201 − 0.002 220*i*	IYZYZIII	0.034 152 − 0.006 215*i*
IIYYIIII	0.047 746 − 0.040 370*i*	IXZXYZYI	0.018 705 − 0.003 404*i*	XZXIIIIZ	0.052 229 − 0.009 504*i*
XZXIIIII	−0.021 561 + 0.077 956*i*	XZZXXXII	−0.016 647 + 0.003 029*i*	ZIIIIYZY	0.030 922 − 0.005 627*i*

TABLE VI. (*Continued.*)

YIYIIIII	0.017 118 − 0.003 115i	IYYIXZZX	0.006 593 − 0.001 200i	XZZXIIII	−0.027 204 + 0.031 862i
IIIIIYZY	−0.012 982 + 0.018 373i	XXIIXZZX	−0.019 254 + 0.003 504i	XZXIIZII	0.011 702 − 0.002 129i
ZIIIIZII	0.102 700 − 0.018 688i	IIIIIZIZ	0.092 214 − 0.016 780i	IIIIIZII	−0.386 698 + 0.100 135i
IYYIIXXI	0.008 283 − 0.001 507i	IIIZIZII	0.105 681 − 0.019 231i	XXIIIIII	0.001 646 − 0.022 572i
IIIIYYXX	0.002 918 − 0.000 531i	IZIZIIII	0.092 214 − 0.016 780i	YZYIZIII	0.040 337 − 0.007 340i
XXXXIIII	0.015 119 − 0.002 751i	XZZXIIXX	−0.029 557 + 0.005 379i	IIIZIIIZ	0.184 425 − 0.033 560i
IIIZIIII	−0.894 071 + 0.367 379i	IIZIIIIZ	0.144 136 − 0.026 228i	IYZYYZYI	0.018 705 − 0.003 404i

APPENDIX C: HOW TO GET COMPLEX EIGENVALUE BY THE DIRECT MEASUREMENT METHOD

If the output state equation (17) is measured many times, the possibility of obtaining the $|0\rangle_a$ state, p, is related to E by the following equation:

$$p = \frac{E^2}{A^2}, \tag{C1}$$

which reveals $|E| = \sqrt{p}A$. To obtain the phase, one way is that we apply a similar circuit for $H'_\theta = xI^{\otimes n} + H_\theta$, where x is a selected real number. Then, the updated U'_r leads us to

$$p' = \frac{|x + Ee^{i\varphi}|^2}{A'^2}. \tag{C2}$$

By applying $|E| = \sqrt{p}A$ to Eq. (C2), we can solve the phase φ and finally the complex eigenvalue as

$$Ee^{i\varphi} = \sqrt{p}Ae^{i\cos^{-1}\frac{p'A'^2 - x^2 - pA^2}{2xA\sqrt{p}}} \; or \sqrt{p}Ae^{-i\cos^{-1}\frac{p'A'^2 - x^2 - pA^2}{2xA\sqrt{p}}}. \tag{C3}$$

If we expand the exponential term in Eq. (C3), it becomes

$$Ee^{i\varphi} = \frac{p'A'^2 - x^2 - pA^2}{2x} + i\frac{\sqrt{(2xA\sqrt{p})^2 - (p'A'^2 - x^2 - pA^2)^2}}{2x}. \tag{C4}$$

Since the measurement errors for p and p', i.e., $\Delta(p)$ and $\Delta p'$, are $O(\frac{1}{\sqrt{N}})$, based on Eq. (C4), the error for the complex eigenvalue $Ee^{i\varphi}$ is

$$\Delta(Ee^{i\varphi}) = O\left(\frac{1}{\sqrt{N}}\right). \tag{C5}$$

The larger the sampling size, the more accurate the obtained complex eigenvalues are.

There are also other choices to obtain the phase. For example, instead of adding the $I^{\otimes n}$ part, we can try building U'_r based on $H_\theta + H_\theta^2$ or $H_\theta + H_\theta^3$ to get an equation such as Eq. (C2) containing phase information. This equation together with Eq. (C1) will reveal the complex eigenvalue for the input eigenstate with another expression.

APPENDIX D: HAMILTONIANS AND EIGENVALUES FOR THE MODEL SYSTEM IN DIFFERENT CASES

1. n = 2 basis functions, 5 qubits

The complex-rotated Hamiltonian of the model system is

$$\begin{aligned} H_\theta = {} & 1.315\,56 * e^{-0.041\,80i}\, II + 0.133\,33 * e^{2.328\,88i}\, YY \\ & + 0.133\,33 * e^{2.328\,88i} XX 0.252\,12 * e^{3.052\,83i}\, ZI \\ & + 1.063\,78 * e^{3.110\,93i}\, IZ. \end{aligned} \tag{D1}$$

By running the circuit shown in Fig. 4 for H_θ and a similar circuit for $H'_\theta = xII + H_\theta$, the complex eigenvalue can be derived by

$$Ee^{i\varphi} = \sqrt{p}Ae^{i\cos^{-1}\frac{p'A'^2 - x^2 - pA^2}{2xA\sqrt{p}}} \; or \; \sqrt{p}Ae^{-i\cos^{-1}\frac{p'A'^2 - x^2 - pA^2}{2xA\sqrt{p}}}, \tag{D2}$$

where A and A' can be obtained from the absolute value of coefficients in H_θ and H'_θ and p and p' can be obtained from the measurement results.

2. n = 2 basis functions, 4 qubits

The complex-rotated Hamiltonian of the model system without the II term is

$$\begin{aligned} H_\theta = {} & 0.133\,33 * e^{2.328\,88i}\, YY + 0.133\,33 * e^{2.328\,88i} XX \\ & + 0.252\,12 * e^{3.052\,83i} ZI + 1.063\,78 * e^{3.110\,93i}\, IZ. \end{aligned} \tag{D3}$$

If we choose $H'_\theta = H_\theta + H_\theta^3$, which has the same terms of tensor products as H_θ with different coefficients, by running Fig. 5, the complex eigenvalue for the original Hamiltonian can be represented by

$$Ee^{i\varphi} = (1.314\,41 - 0.054\,97i) + \sqrt{p}Ae^{\frac{i}{2}\cos^{-1}\left(\frac{p'A'^2}{2p^2A^4} - \frac{1}{2pA^2} - \frac{pA^2}{2}\right)} \tag{D4}$$

or

$$(1.314\,41 - 0.054\,97i) + \sqrt{p}Ae^{\frac{-i}{2}\cos^{-1}\left(\frac{p'A'^2}{2p^2A^4} - \frac{1}{2pA^2} - \frac{pA^2}{2}\right)}, \tag{D5}$$

where A and A' can be obtained from the absolute value of coefficients in H_θ and H'_θ and p and p' can be obtained from the measurement results.

3. n = 2 basis functions, 3 qubits

The square of the Hamiltonian in Eq. (D3) is

$$H_\theta^2 = 1.195\,77 * e^{-0.097\,23i} II + 0.535\,29 * e^{-0.053\,11i} ZZ. \tag{D6}$$

If we choose $(H_\theta^2)' = H_\theta^2 + H_\theta^4$, by running Fig. 6, the complex eigenvalue for the original Hamiltonian is

$$Ee^{i\varphi} = (1.314\,41 - 0.054\,97i) + p^{\frac{1}{4}}\sqrt{A}e^{\frac{i}{2}\cos^{-1}\left(\frac{p'A'^2}{2p^{\frac{3}{2}}A^3} - \frac{1}{2\sqrt{p}A} - \frac{\sqrt{p}A}{2}\right)} \tag{D7}$$

or

$$(1.314\,41 - 0.054\,97i) + p^{\frac{1}{4}}\sqrt{A}e^{\frac{-i}{2}\cos^{-1}\left(\frac{p'A'^2}{2p^{\frac{3}{2}}A^3} - \frac{1}{2\sqrt{p}A} - \frac{\sqrt{p}A}{2}\right)}, \tag{D8}$$

where A and A' can be obtained from the absolute value of coefficients in H_θ^2 and $H_\theta^2 + H_\theta^4$ and p and p' can be obtained from their measurement results.

APPENDIX E: QUANTUM CIRCUIT FOR COMPLEX-SCALED HAMILTONIAN OF H_2^- AT $\theta = 0.18$, $\alpha = 1.00$

The complex-scaled Hamiltonian of H_2^- at $\theta = 0.18$, $\alpha = 1.00$ in Appendix B can be written as

$$\begin{aligned} H = {} & 0.019\,012 * e^{-0.180\,013i} IXZXXZXI + 0.038\,818 \\ & * e^{-0.180\,010i} IIIZIXZX + 0.105\,638 * e^{-0.180\,005i} ZIZIIIII \\ & + 0.028\,282 * e^{-0.179\,983i} XZXIXZXI + \cdots \\ & + 0.019\,012 * e^{-0.180\,013i} IYZYYZYI. \end{aligned} \tag{E1}$$

We would like to mention that the terms explicitly shown in Eq. (E1) are following the order in Appendix B. It is a coincident that their

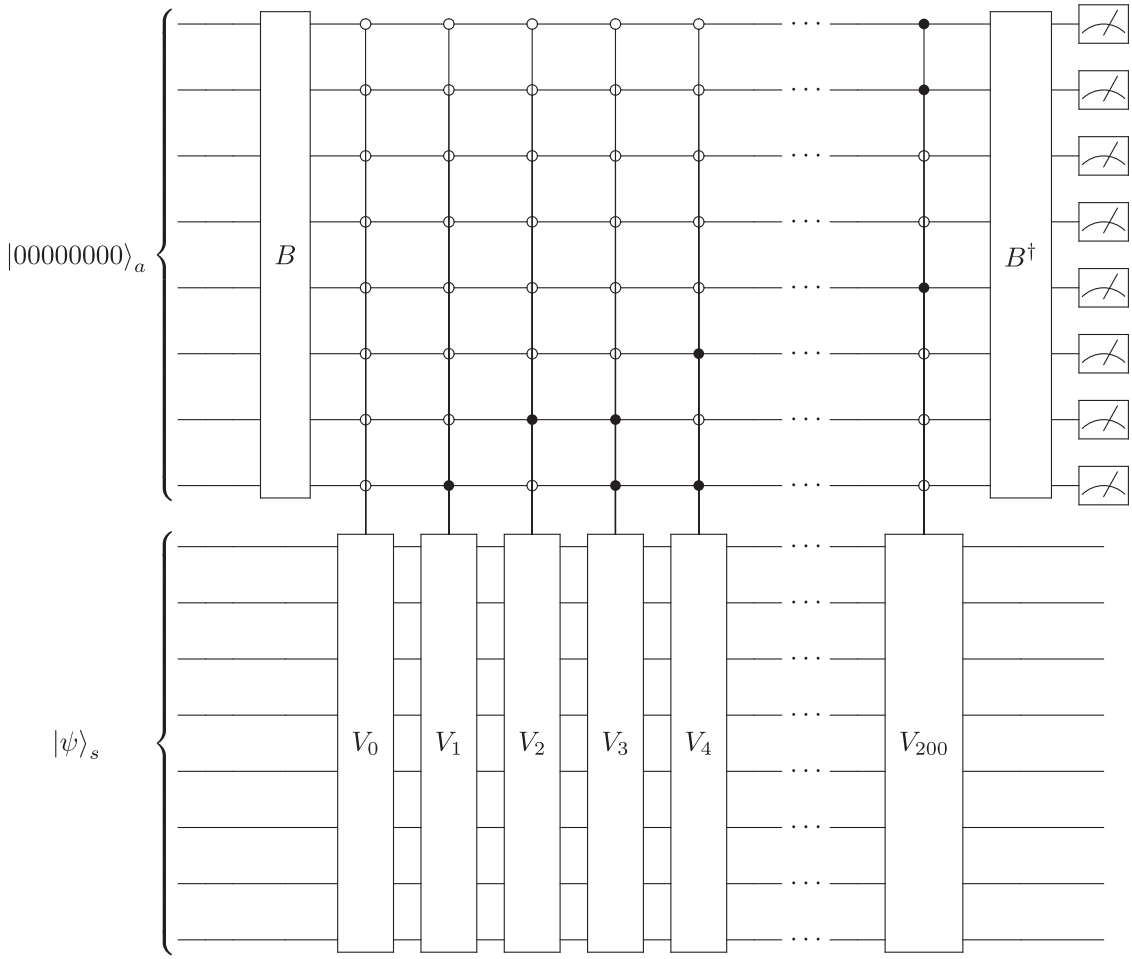

FIG. 8. The quantum circuit to run the direct measurement method for H_2^- when $\theta = 0.18$, $\alpha = 1.00$. The B gate can be prepared by $\boldsymbol{\beta}$ in Eq. (E2). V_i gates are listed in Eq. (E3).

phases are similar. For example, one term we did not show in the Hamiltonian is $0.021\,284 * e^{1.542\,696i} IIIIYYII$, which has a different phase.

To construct the quantum circuit for the direct measurement method, we need to create the B gate and V gate. The B gate can be prepared by the coefficients from the Hamiltonian in Eq. (E1),

$$\beta = \begin{matrix} index \\ 0 \\ 1 \\ 2 \\ 3 \\ \vdots \\ 200 \\ 201 \\ 202 \\ \vdots \\ 255 \end{matrix} \begin{bmatrix} 0.019012 \\ 0.038818 \\ 0.105638 \\ 0.028282 \\ \vdots \\ 0.019012 \\ 0 \\ 0 \\ \vdots \\ 0 \end{bmatrix}, \tag{E2}$$

as shown in Eq. (15). The V gate can be constructed by a series of controlled-V_i gates, where V_i are

$$\begin{aligned} V_0 &= e^{-0.180\,013i} IXZXXZXI, \\ V_1 &= e^{-0.180\,010i} IIIZIXZX, \\ V_2 &= e^{-0.180\,005i} ZIZIIIII, \\ V_3 &= e^{-0.179\,983i} XZXIXZXI, \\ &\vdots \\ V_{200} &= e^{-0.180\,013i} IYZYYZYI. \end{aligned} \tag{E3}$$

The whole circuit is shown in Fig. 8. The encoding of control qubits is based on the binary form of V_i's index i. For example, V_3 is applied to $|\psi\rangle_s$ if the ancilla qubit state is $|3\rangle_a = |000\,000\,11\rangle_a$.

DATA AVAILABILITY

The data that support the findings of this study are available from the corresponding author upon reasonable request.

REFERENCES

[1] W. P. Reinhardt, "Complex coordinates in the theory of atomic and molecular structure and dynamics," Annu. Rev. Phys. Chem. **33**, 223–255 (1982).
[2] J. Aguilar and J. M. Combes, "A class of analytic perturbations for one-body Schrödinger Hamiltonians," Commun. Math. Phys. **22**, 269–279 (1971).
[3] E. Balslev and J. M. Combes, "Spectral properties of many-body Schrödinger operators with dilatation-analytic interactions," Commun. Math. Phys. **22**, 280–294 (1971).
[4] B. Simon, "Quadratic form techniques and the Balslev-Combes theorem," Commun. Math. Phys. **27**, 1–9 (1972).
[5] B. Simon, "Resonances in n-body quantum systems with dilatation analytic potentials and the foundations of time-dependent perturbation theory," Ann. Math. **97**, 247–274 (1973).
[6] C. van Winter, "Complex dynamical variables for multiparticle systems with analytic interactions. I," J. Math. Anal. Appl. **47**, 633–670 (1974).
[7] N. Moiseyev, "Quantum theory of resonances: Calculating energies, widths and cross-sections by complex scaling," Phys. Rep. **302**, 212–293 (1998).
[8] N. Moiseyev and C. Corcoran, "Autoionizing states of H_2 and H_2^- using the complex-scaling method," Phys. Rev. A **20**, 814 (1979).
[9] A. Emmanouilidou and L. E. Reichl, "Scattering properties of an open quantum system," Phys. Rev. A **62**, 022709 (2000).
[10] Y. Orimo, T. Sato, A. Scrinzi, and K. L. Ishikawa, "Implementation of the infinite-range exterior complex scaling to the time-dependent complete-active-space self-consistent-field method," Phys. Rev. A **97**, 023423 (2018).
[11] T.-C. Jagau, "Coupled-cluster treatment of molecular strong-field ionization," J. Chem. Phys. **148**, 204102 (2018).
[12] I. Haritan and N. Moiseyev, "On the calculation of resonances by analytic continuation of eigenvalues from the stabilization graph," J. Chem. Phys. **147**, 014101 (2017).
[13] A. Landau, A. Ben-Asher, K. Gokhberg, L. S. Cederbaum, and N. Moiseyev, "*Ab initio* complex potential energy curves of the $He^*(1s2p^1p)$–Li dimer," J. Chem. Phys. **152**, 184303 (2020).
[14] D. Bhattacharya, A. Landau, and N. Moiseyev, "*Ab initio* complex transition dipoles between autoionizing resonance states from real stabilization graphs," J. Phys. Chem. Lett. **11**, 5601–5609 (2020).
[15] A. Pick, P. R. Kaprálová-Žďánská, and N. Moiseyev, "*Ab-initio* theory of photoionization via resonances," J. Chem. Phys. **150**, 204111 (2019).
[16] N. Moiseyev, P. R. Certain, and F. Weinhold, "Complex-coordinate studies of helium autoionizing resonances," Int. J. Quantum Chem. **14**, 727–736 (1978).
[17] S. Kais and D. R. Herschbach, "Dimensional scaling for quasistationary states," J. Chem. Phys. **98**, 3990–3998 (1993).
[18] T. C. Germann and S. Kais, "Large order dimensional perturbation theory for complex energy eigenvalues," J. Chem. Phys. **99**, 7739–7747 (1993).
[19] S. Kais, *Quantum Information and Computation for Chemistry*, Advances in Chemical Physics Vol. 154 (Wiley Online Library, NJ, 2014), p. 224109.
[20] R. Xia and S. Kais, "Quantum machine learning for electronic structure calculations," Nat. Commun. **9**, 4195 (2018).
[21] T. Bian, D. Murphy, R. Xia, A. Daskin, and S. Kais, "Quantum computing methods for electronic states of the water molecule," Mol. Phys. **117**, 2069–2082 (2019).
[22] A. Daskin, T. Bian, R. Xia, and S. Kais, "Context-aware quantum simulation of a matrix stored in quantum memory," Quantum Inf. Process. **18**, 357 (2019).
[23] R. Xia, T. Bian, and S. Kais, "Electronic structure calculations and the Ising Hamiltonian," J. Phys. Chem. B **122**, 3384–3395 (2017).
[24] S. Lloyd, "Universal quantum simulators," Science **273**, 1073–1078 (1996).
[25] A. Daskin, A. Grama, and S. Kais, "A universal quantum circuit scheme for finding complex eigenvalues," Quantum Inf. Process. **13**, 333–353 (2014).
[26] G. Aleksandrowicz *et al.*, "Qiskit: An open-source framework for quantum computing," (accessed on March 16, 2019).
[27] N. Moiseyev, *Non-Hermitian Quantum Mechanics* (Cambridge University Press, 2011).
[28] N. Moiseyev, P. R. Certain, and F. Weinhold, "Resonance properties of complex-rotated Hamiltonians," Mol. Phys. **36**, 1613–1630 (1978).

[29]G. D. Doolen, "A procedure for calculating resonance eigenvalues," J. Phys. B: At. Mol. Phys. **8**, 525 (1975).
[30]J. T. Seeley, M. J. Richard, and P. J. Love, "The Bravyi-Kitaev transformation for quantum computation of electronic structure," J. Chem. Phys. **137**, 224109 (2012).
[31]P. J. J. O'Malley, R. Babbush, I. D. Kivlichan, J. Romero, J. R. McClean, R. Barends, J. Kelly, P. Roushan, A. Tranter, N. Ding *et al.*, "Scalable quantum simulation of molecular energies," Phys. Rev. X **6**, 031007 (2016).
[32]A. Aspuru-Guzik, A. D. Dutoi, P. J. Love, and M. Head-Gordon, "Simulated quantum computation of molecular energies," Science **309**, 1704–1707 (2005).
[33]Y. Cao, J. Romero, J. P. Olson, M. Degroote, P. D. Johnson, M. Kieferová, I. D. Kivlichan, T. Menke, B. Peropadre, N. P. D. Sawaya *et al.*, "Quantum chemistry in the age of quantum computing," Chem. Rev. **119**, 10856–10915 (2019).
[34]J. McClean, N. Rubin, K. Sung, I. David Kivlichan, X. Bonet-Monroig, Y. Cao, C. Dai, E. S. Fried, G. Gidney, B. Gimby *et al.*, "OpenFermion: The electronic structure package for quantum computers," Quantum Sci. Technol. **5**, 034014 (2020).
[35]A. Daskin and S. Kais, "Direct application of the phase estimation algorithm to find the eigenvalues of the Hamiltonians," Chem. Phys. **514**, 87–94 (2018).
[36]R. Ellerbrock and T. J. Martinez, "A multilayer multi-configurational approach to efficiently simulate large-scale circuit-based quantum computers on classical machines," J. Chem. Phys. **153**, 051101 (2020).
[37]Y. Zhou, E. Miles Stoudenmire, and X. Waintal, "What limits the simulation of quantum computers?," Phys. Rev. X **10**, 041038 (2020).